CENTRE FOR ELECTRON MICROSCOPY AND MICROANALYSIS (CEMM)

The Centre for Electron Microscopy and Microanalysis (CEMM) is an instrumental centre at the JSI that combines analytical equipment in the field of electron microscopy and microanalysis. Access to the research equipment of CEMM is provided to other JSI departments as well as other research institutions, universities and industrial partners. The equipment at the CEMM is used by researchers, interested in the morphology and structural and chemical characterization of materials between the micrometre and the atomic levels. At the CEMM there are currently two scanning electron microscopes (SEM) JSM-5800 and JSM-7600F, two transmission electron microscopes (TEM) JEM-2100 (CO NiN) and JEM-2010F, and the equipment for the TEM and SEM sample preparation. Centre of Excellence NAMASTE contributed to the equipment for electron microscopy a CCD camera and an ADF (annular dark field) detector for JEM-2010F microscope and an EBSD system for the JSM-7600F. Additionally, the IJS is a co-owner (20%) of a JEM ARM 200CF (transmission electron microscope with atomic resolution) at the Chemical Institute. Furthermore, CEMM helps with the maintenance of the FIB (focused ion beam) microscope Helios Nanolab 650 at the Nanocenter Centre of excellence.

At the end of 2019, the equipment of the CEMM was upgraded with a new high-level high-resolution scanning electron microscope Verios G4 HP (Thermo Fisher Scientific). This type of a microscope, with extreme high resolution at low accelerating voltages, is unique in this part of the Europe. Furthermore, besides EDSX detector, microscope is equipped with the last developed detector for transmission microscopy (STEM). Microscope will be installed and ready to use in the middle of the 2020.

The research involving the staff and equipment at the CEMM is diverse regarding the investigated materials and the methods used.

- Scanning electron microscopy is employed to observe the morphology and structure of the surfaces and for the microstructural investigation and determination of the chemical composition. Samples that are mostly investigated are ceramics (polycrystalline oxide and non-oxide compositions), nanostructured materials, metallic magnetic materials, metals, alloys glass, etc. All of the scanning electron microscopes in the CEMM are equipped with an energy-dispersion (EDXS) and / or wavelength dispersion (WDXS) spectrometer for X-rays, allowing non-destructive determination of the chemical composition of the investigated materials. The scanning electron microscope JSM-7600F is additionally equipped with an electron back-scattered diffraction (EBSD) detector and an electron lithography system.
- Transmission electron microscopy (TEM) provides an insight into the structure of the material on the nano-scale (atomic level). Transmission electron microscopy enables structural and chemical analyses of the grain boundaries and study of precipitates, planar defect and dislocation determination. Additionally, to ceramic samples also other materials and structures are investigated such as thin films on different substrates, alloys, delicate metallic magnetic materials, polymers, etc. Transmission electron microscope JEM-2100 is equipped with an EDXS spectrometer and a CCD camera, and the JEM-2010F is additionally equipped with a scanning transmission electron (STEM) unit, EDXS and EELS (electron energy loss) spectrometers, and a CCD camera.
- The CEMM also manages the necessary equipment for the SEM and TEM sample preparation.

The operation of the Centre is managed by properly trained employees. Besides maintenance of the equipment, other CEMM activities include, among other, training of new operators (Figure 1), organization of workshops and conferences on the topic of electron microscopy, providing services for industrial partners and implementation of new analytical techniques. CEMM personnel are also responsible for the dissemination of electron microscopy techniques to the general public in the scope of organized visits to the IJS, as well through publications in traditional and digital media (Figure 2).

In 2019 the CEMM organized the 8th and 9th workshop (SEM sample preparation and scanning electron microscopy with microanalysis- EDXS) for users of the CEMM equipment. The aim of the workshops was to explain the operation and handling of the equipment.

Figure 1. Training of new operators.

Figure 2. Organisation of experiments for the JSI visitors.

Examples of microstructural and nanostructural investigations using the CEMM equipment

The examples of analyses of structural and chemical characterisations of different materials using electron microscopy techniques were performed by the CEMM employees as well as operators from different JSI departments.

1. Heating experiment in TEM

Heating experiment of $BaTiO_3$ doped with metal Ni was performed in a transmission electron microscope JEM-2100. Experiments were conducted within the temperature range of the phase transformation at ~120°C. The study of heating experiment was aimed: (a) to show phase transformation from tetragonal to cubic $BaTiO_3$, (b) to identify structural defects (domains or twins of tetragonal $BaTiO_3$) and (c) to investigate the nature of grain boundaries between $BaTiO_3$ and Ni (Figure 3) (Zajc I., K8; Drev S., CEMM).

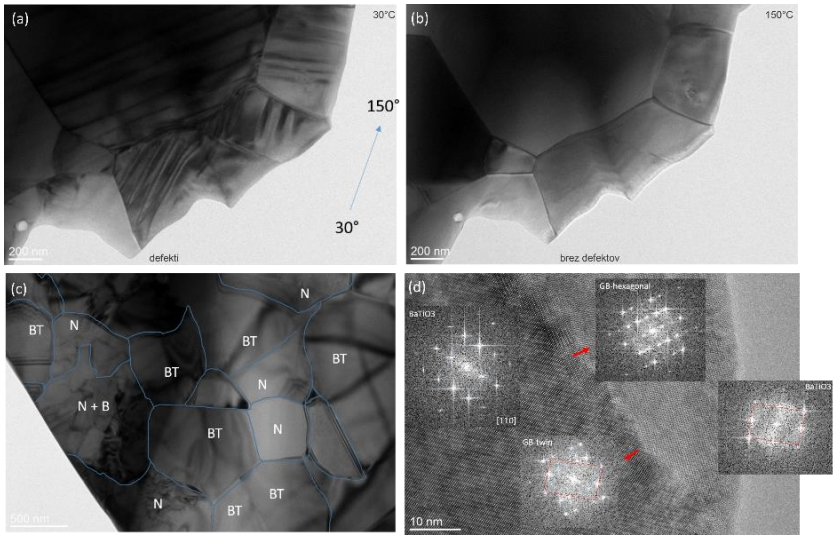

Figure 3. TEM analysis of grain boundaries between $BaTiO_3$ and metal Ni. (a,b) Heating experiment showing transformation from tetragonal to cubic structure. (c) Grain boundaries between $BaTiO_3$ and Ni and (d) SAED of bulk and boundary region (Zajc I., K8, Drev S., CEMM, JEM 2100).

2.Electrochemical *in-situ* experiment in TEM

In a field of electrochemistry, we performed *in-situ* experiments of electrochemical deposition of metal Ni on Pt work electrode during potential cycling between the work electrode and the cathode (Figure 4) (Koblar M., Drev S., CEMM).

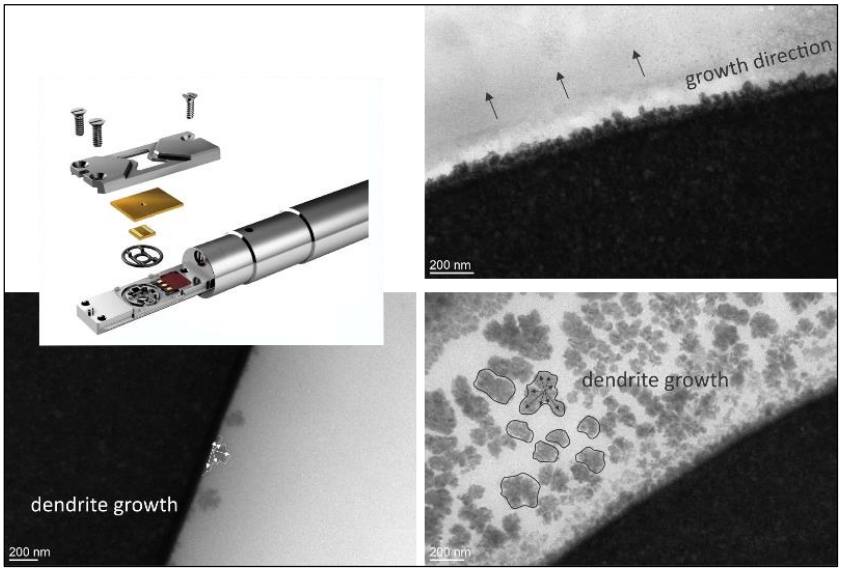

Figure 4. (a) Liquid cell in TEM. (b,c,d) Dendritic growth of Ni from solution observed on the Pt work electrode (Koblar M., Drev S., CEMM, JEM 2100).

3. Titanium oxynitride structure

TEM analysis of anatase nanotube sintered in NH_3 atmosphere. SAED study of anatase nanotubes confirmed phase transformation from anatase to titanium oxynitride (Figure 5).

In: Suhadolnik. L.; Jurković. L. D.; Likozar. B; Bele. M.; Drev. S.; Čeh. M. Structured titanium oxynitride (TiO_xN_y) nanotube arrays for a continuous electrocatalytic phenol-degradation process: Synthesis, characterisation, mechanisms and the chemical reaction micro-kinetics. Applied Catalysis B: Environmental, 2019, 257, 117894-117904

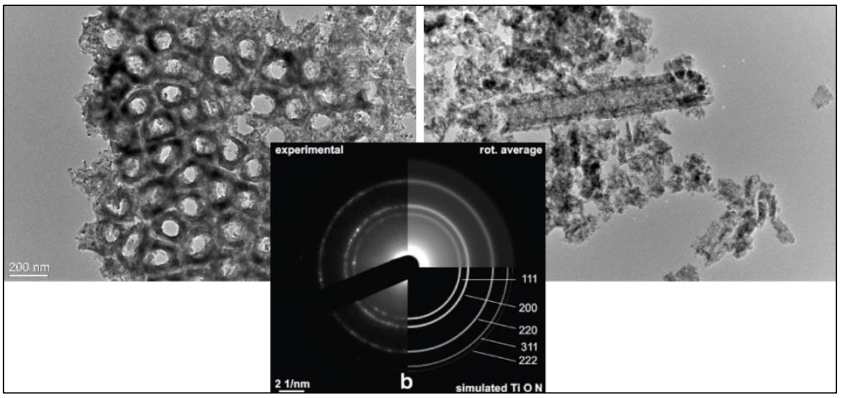

Figure 5. BF TEM image of Ti-O-N sample with the corresponding SAED pattern, demonstrating phase transformation of TiO_2 anatase to Ti-O-N phase (Drev S., CEMM, JEM 2010F).

4. Ferroelastic domains in sintered perovskite ceramics

TEM analysis of ferro elastic domains in spark-plasma sintered $Na(Nb_{0.2}Ta_{0.8})O_3$ perovskite ceramics, crystallized with *Pcmn* orthorhombic symmetry. Superstructure reflections from doubling of the unit cell revealing rotation of oxygen octahedral in structure (Figure 6).

In: Bian. J.J.; Otoničar. M.; Spreitzer. M.; Vengust. D.; Suvorov. D. Structural evolution, dielectric and energy storage properties of Na ($Nb_{1-x}Ta_x)O_3$ ceramics prepared by spark plasma sintering. Journal of the European Ceramic Society, 2007, 39, 2339-2347

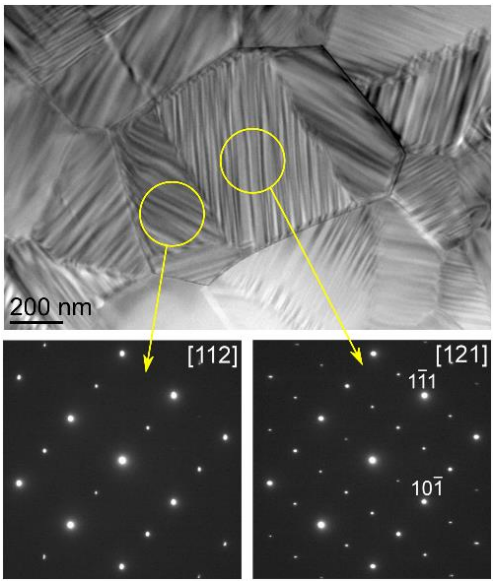

Figure 6. Analysis of ferro elastic domains in $Na(Nb_{0.2}Ta_{0.8})O_3$ perovskite ceramics (Otoničar M., K5, JEM 2100).

5. $(Nd,Na)(SO_4)_2$ x H_2O crystals

Analysis and study of grain growth and morphological characterisation of $(Nd,Na)(SO_4)_2$ x H_2O has been performed in a scanning electron microscope (Figure 7).

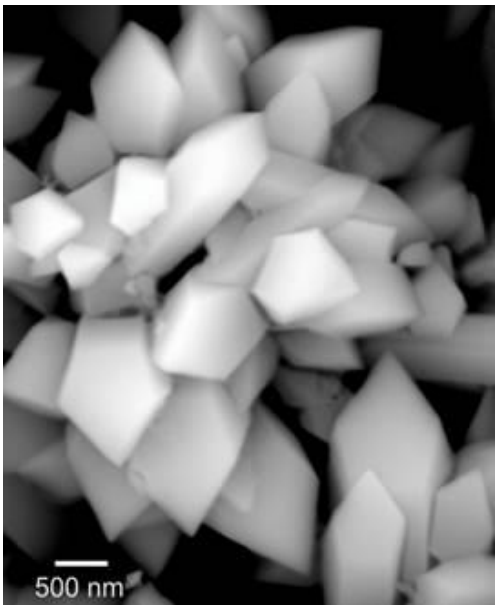

Figure 7. $(Nd,Na)(SO_4)_2$ x H_2O crystals (Xu. X., Samardžija Z., K7, JSM 7600F).

6. Al_2O_3/Ru magnetic sample

Magnetic samples based on Al_2O_3/Ru were analysed by transmission electron microscopy. Samples are composed of aluminium oxide grains that are surrounded with Ru nanoparticles (Figure 8).

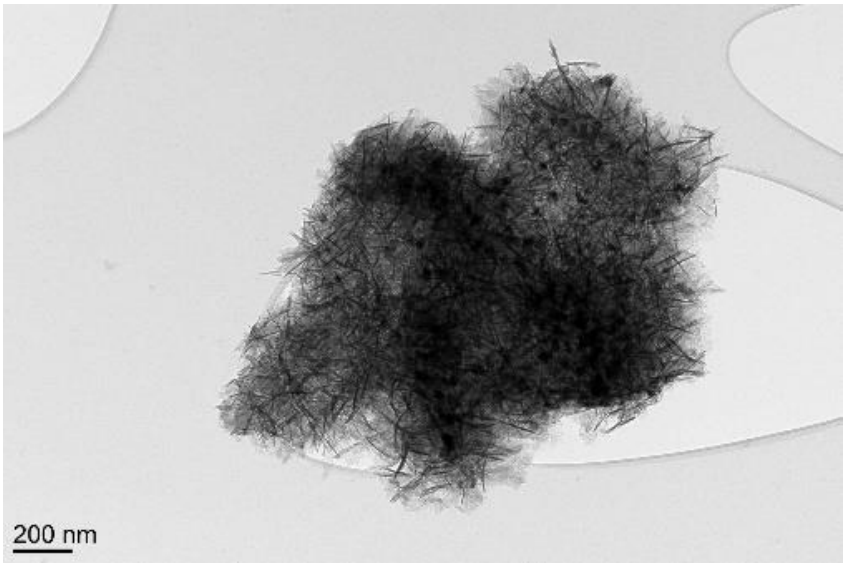

Figure 8. TEM image of the Ru nanoparticles-decorated magnetic alumina catalyst (Gyergyek S., K8, JEM 2100).

7. SnO_2 ceramics

Analysis of thermal etching SnO ceramics doped with CoO and NB_2O_5 showed the appearance of many twins in SnO_2 grains in (101) planes (Figure 9).

In: Tominc. S.; Rečnik. A.; Samardžija. Z.; Dražić. G.; Podlogar. M.; Bernik. S.; Daneu. N. Twinning and charge compensation in Nb_2O_5-doped SnO_2-CoO ceramics exhibiting promising varistor characteristics. Ceramics international, 2018, 44, 1603-1613

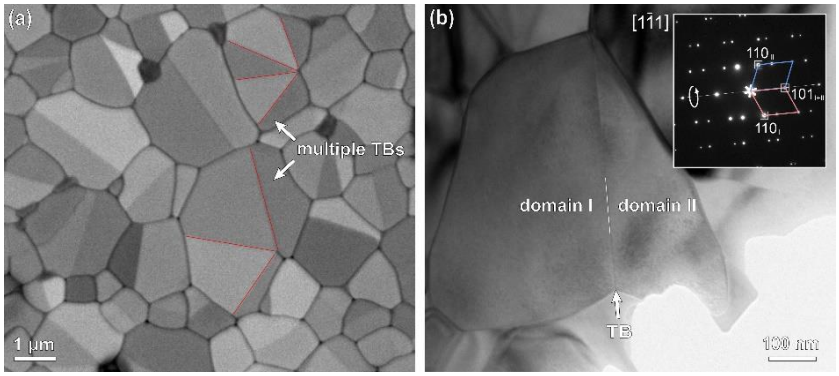

Figure 9. (a) SEM/BSE image of thermally etched cross-section of SnO_2-based ceramics doped with CoO and Nb_2O_5 shows abundant formation of twins in SnO_2 grains. Different shades of BSE contrast are due to different orientations of SnO_2 grains. (b) TEM analysis revealed that twins lie in (101) planes of the SnO_2 structure (Tominc S., K7, Rečnik A., K7, Daneu N., K9, JSM 7600F, JEM 2100).

8. Mn-oxide nanoparticles

High resolution image of Mn-oxide nanoparticles revealed orientation along [131] zone (Figure 10).

In: Ristić. A.;Mazaj. M.; Arčon. I.; Daneu. N.; Zabukovec. L. N.; Gläser. R.; Novak. T. N. New insights into manganese local environment in MnS-1 nanocrystals. Crystal Growth and Design, 2019, 19, 3130-3138

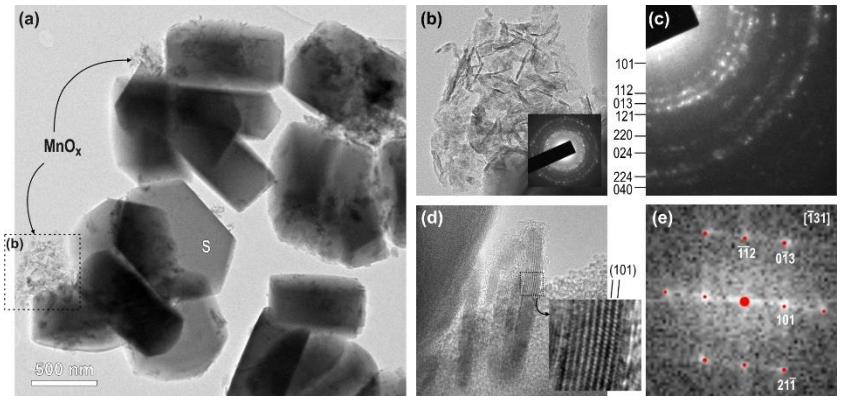

Figure 10. (a) Mn-oxide nanoparticles on zeolite silicalite-1 (S-1) with MFI structure. (b,c) The nanoparticles are hausmannite (Mn_3O_4) as revealed by SAED. (d) HRTEM image and (e) indexed FF pattern of the rod-shaped crystallite oriented along [-131] zone axis (Daneu N., K9, JEM 2100).

9. $Bi_4Ti_3O_{12}$ transformation

Within the research project of the study mechanism of transformation of $Bi_4Ti_3O_{12}$ nanoparticles in $SrTiO_3$ nanoplatelets (M.ERA-NET 3184 HarvEnPiez; leader dr. Marjeta Maček Kržmanc) analysis of mechanism of topochemical transformation $Bi_4Ti_3O_{12}$ (BIT) to $SrTiO_3$ (STO) under hydrothermal conditions has been done. Analysis showed BIT platelets terminated with $Bi_2O_2^{2+}$ layer, starts at the edges and proceeds towards the interior of the plate (Figure 11).

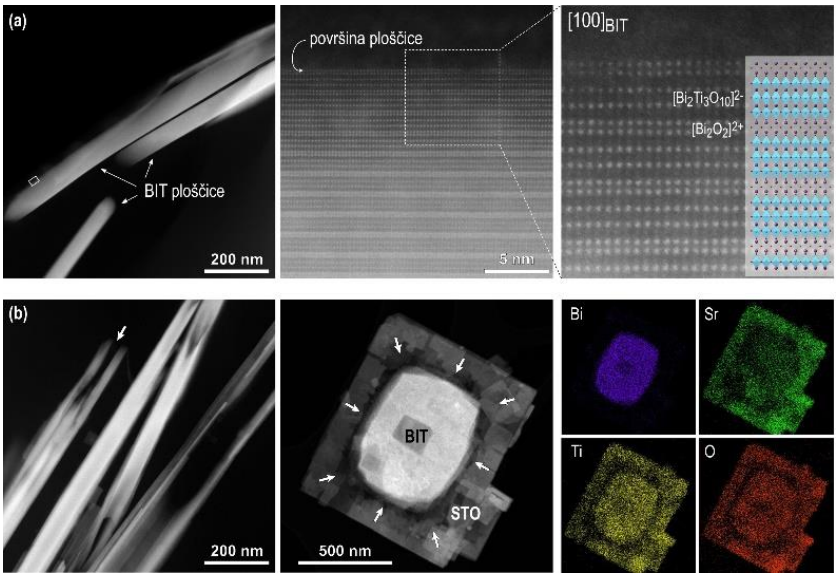

Figure 11. TEM study of the mechanism of topochemical transformation of $Bi_4Ti_3O_{12}$ (BIT) to $SrTiO_3$ (STO) (a) Initial BIT nanoplatelets have atomically flat surface and are $Bi_2O_2^{2+}$ terminated. (b) Analysis of partially transformed BIT platelets to STO shows that the transformation starts at the edges and proceeds towards the interior of the plate (Daneu N., K9, ARM 200F).

EMPLOYEES

Researcher

1. **Prof. Miran Čeh, head**

Postdoctoral coworkers

2. Dr. Sandra Drev
3. Dr. Jitka Hreščak

Young researcher

4. Andreja Šestan Zavašnik

Technical assistant:

5. Maja Koblar, univ. dipl. fiz.